



**THE USE OF X-RAY PULSARS
FOR SPACECRAFT NAVIGATION**

Suneel I. Sheikh, Darryll J. Pines, Paul S. Ray, Kent S. Wood,
Michael N. Lovellette, and Michael T. Wolff

**14th AAS/AIAA Space Flight
Mechanics Conference**

Maui, Hawaii,

February 8-12, 2004

AAS Publications Office, P.O. Box 28130, San Diego, CA 92198

THE USE OF X-RAY PULSARS FOR SPACECRAFT NAVIGATION

Suneel I. Sheikh[†], Darryll J. Pines^{††}, Paul S. Ray[✉], Kent S. Wood[‡],
Michael N. Lovellette[§], and Michael T. Wolff^{§§}

This paper presents a novel technique for determining spacecraft time, position, velocity, and attitude using celestial X-ray sources, such as pulsars. Pulsars are rapidly rotating neutron stars that generate electromagnetic radiation that can be detected in the radio, infrared, visible, ultraviolet, X-ray, and gamma-ray bands. Many pulsars appear as unique, periodic, and stable sources, similar to lighthouses used for ship navigation. Empirical models can be created to predict the pulse arrival time from pulsars within a reference inertial frame. In this paper, an overview of pulsars is presented, along with the characteristics of these sources that make them useful for navigation. Methods are developed to illustrate how X-ray pulsars might be used for 3-D position determination. An example is provided to show how observed data is used to determine position.

INTRODUCTION

Most space vehicle operations rely heavily on Earth-based navigation solutions to complete their tasks (Refs. 1, 2, and 3). As the cost of vehicle operations continues to increase, spacecraft navigation is evolving away from Earth-based solutions towards increasingly autonomous methods (Refs. 4 and 5). For vehicles operating near Earth, the current Global Positioning System (GPS) can provide a complete navigation solution comprised of referenced time, position, and attitude. However, these human-developed systems have limited scope for operations of vehicles relatively far from Earth. Thus, an autonomous celestial-based system, which uses sources at great distance from Earth that can provide a complete navigation solution for spacecraft missions, remains attractive. Recently discovered celestial sources may provide answers to navigating throughout the solar system and beyond. Neutron stars, found to be spinning at exceptionally fast rates, with immense magnetic fields, and referred to as *pulsars*, provide a stable, predictable, unique signature. This paper presents further investigation into the utilization of pulsar sources, specifically those emitting in the X-ray band, as navigation aides for spacecraft.

[†] Doctoral Candidate, Aerospace Engineering, Building 382, University of Maryland, College Park, Maryland 20742. Email: sheikh@ssl.umd.edu. Phone: 301-405-4454, FAX: 301-405-2918. Web site: <http://www.ssl.umd.edu>.

^{††} Associate Professor, Aerospace Engineering, Room 3154 Martin Hall, University of Maryland, College Park, Maryland 20742. Email: djpterp@eng.umd.edu. Phone: 301-405-0263, FAX: 301-314-9001. Web site: <http://www.ena.umd.edu>.

[✉] Astrophysicist, Space Science Division, Naval Research Laboratory, Code 7655, 4555 Overlook Ave., SW, Washington, District of Columbia, 20375. Email: Paul.Ray@nrl.navy.mil. Phone: 202-404-1619. FAX: 202-767-0497. Web site: <http://xweb.nrl.navy.mil>.

[‡] Head UV/X-ray Astrophysics and Analysis Section, Space Science Division, Naval Research Laboratory, Code 7655, 4555 Overlook Ave., SW, Washington, District of Columbia, 20375. Email: kent.wood@nrl.navy.mil. Phone: 202-767-2506. FAX: 202-767-0497. Web site: <http://xweb.nrl.navy.mil>.

[§] Physicist, Space Science Division, Naval Research Laboratory, Code 7655, 4555 Overlook Ave., SW, Washington, District of Columbia, 20375. Email: lovellette@xip.nrl.navy.mil. Phone: 202-404-7460. FAX: 202-767-0497. Web site: <http://xweb.nrl.navy.mil>.

^{§§} Astrophysicist, Space Science Division, Naval Research Laboratory, Code 7655, 4555 Overlook Ave., SW, Washington, District of Columbia, 20375. Email: Michael.Wolff@nrl.navy.mil. Phone: 202-404-7597. FAX: 202-767-0497. Web site: <http://xweb.nrl.navy.mil>.

PULSAR DESCRIPTION

A neutron star is the remnant of a massive star that has exhausted its nuclear fuel and undergone a supernova explosion. The amount of mass not ejected during the supernova determines whether the resulting stellar remnant will be a neutron star or black hole. If the remaining mass is near 1.4 solar masses, the remnant will collapse onto itself and form a neutron star. This star is a small, extremely dense object roughly 20 km in diameter, and is an equilibrium configuration in which nuclear effects provide support against the strong gravity. To reach this allowed equilibrium configuration the stellar constituents must be adjusted by reactions that replace electrons and protons with neutrons, hence the name *neutron stars*. From conservation of angular momentum, during the collapse phase the rotation rate of the star increases. Young, newly born neutron stars typically rotate with periods on the order of tens of milliseconds while older neutron stars eventually slow down to periods on the order of a several seconds. A unique aspect of this rotation is that it can be extremely stable and predictable.

In addition to maintaining stable rotation periods, neutron stars harbor immense magnetic fields. Under the influence of these strong fields, charged particles are accelerated along the field lines to very high energies. As these charged particles move in the pulsar's strong magnetic field, powerful beams of electromagnetic waves are radiated out from the magnetic poles of the star. If the neutron star's spin axis is not aligned with its magnetic field axis, then an observer will sense a *pulse* of electromagnetic radiation as the magnetic pole sweeps across the observer's line of sight to the star. Neutron stars that exhibit this behavior are referred to as *pulsars*. Since no two neutron stars are formed in exactly the same manner or have the same geometric orientation relative to Earth, the pulse frequency and shape produce a unique identifying signature for each pulsar. Thus, pulsars can act as natural beacons, or *celestial lighthouses*, on an intergalactic scale. Figure 1 provides a diagram of a neutron star with its distinct spin and magnetic axes.

In 1967, Cambridge University professor Anthony Hewish and graduate student Jocelyn Bell discovered radio pulsations during an interplanetary scintillation study in the radio frequency of 81.5 MHz (Ref. 6). Among the expected random noise emerged signals timed at regularly spaced intervals, having a period of about 1.337 seconds and constant to better than one part in 10^7 . It was soon realized that these objects were rotating neutron stars pulsating at radio frequencies. Since their discovery, pulsars have been found to emit at the radio, infrared, visible (optical), ultraviolet, X-ray, and gamma-ray bands of the electromagnetic spectrum. There are now ~1200 known pulsars within the Galaxy (Ref. 7). Figure 2 shows an image of the Crab Nebula and Pulsar taken by NASA's *Chandra X-ray Observatory*.

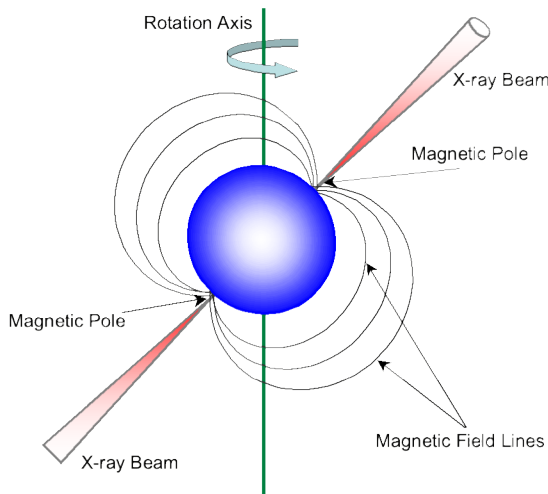


Figure 1. Neutron Star with Rotation Axis and Magnetic Field.

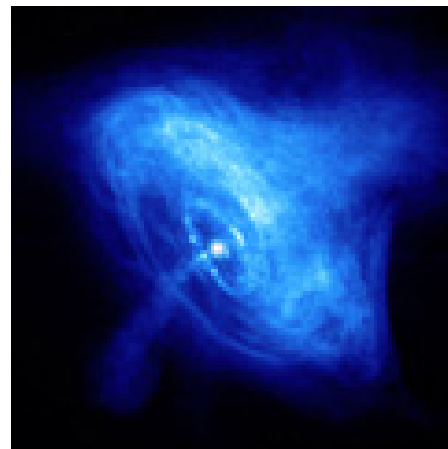


Figure 2. Crab Nebula and Pulsar in X-rays. NASA *Chandra X-ray Observatory*. (NASA/CXC/ASU/J.Hester et al., Ref. 8)

History of Pulsar-Based Navigation

In 1974, Downs (Ref. 9) presented a method of navigation for orbiting spacecraft based upon radio signals from a pulsar. However, both the radio and optical signatures from pulsars have limitations for spacecraft navigation. At the radio frequencies that pulsars emit (~ 100 MHz to few GHz) and with their faint emissions, radio-based systems would require large antennas (on the order of 25 m in diameter or larger) to detect sources, which would be impractical for most spacecraft. Also, many celestial objects and the galactic diffuse emission are broadband radio sources that could obscure weak pulsar signals (Ref. 10). Furthermore, the low signal intensity from radio pulsars would require long signal integration times for an acceptable signal-to-noise ratio. The small population of pulsars with detected optical pulsations (only five isolated pulsars, Ref. 11) severely limits an optical pulsar-based navigation system. Since optical pulsars are also dim sources, large aperture telescopes are required to collect sufficient photons. Any nearby bright visible sources would require precise pointing and significant processing to detect these pulsars.

During the 1970s, astronomical observations within the X-ray band of 1–20 keV (2.5×10^{17} – 4.8×10^{18} Hz) yielded pulsars with X-ray signatures. Chester and Butman (Ref. 12) proposed using pulsars emitting in the X-ray band as an improved option for navigation. Sensors potentially on the order of 0.1 m^2 could be used for X-ray detection, more reasonable for spacecraft than large optical telescopes or radio antennas.

During the early 1990s, Wood (Ref. 13) proposed studying a comprehensive approach to X-ray navigation covering attitude, position, and time, along with a supporting demonstration mission. This study included utilizing X-ray sources other than pulsars. Hanson (Ref. 14) continued this effort, whose thesis in 1996 included a detailed description of spacecraft attitude determination and a method to incorporate time from X-ray sources. From 1999–2000, the Naval Research Laboratory's (NRL) Unconventional Stellar Aspect (USA) experiment onboard the Advanced Research and Global Observation Satellite (*ARGOS*) provided a platform for pulsar-based spacecraft navigation experimentation (Refs. 15, 16, and 17).

X-ray Source Properties

Many X-ray pulsars are *rotation-powered* pulsars, which are isolated neutron stars whose energy source is the stored rotational kinetic energy of the star itself. In addition to these rotation-powered pulsars, two other types of pulsars, *accretion-powered* and *anomalous*, exist that are powered by different energy sources. Accretion-powered pulsars are neutron stars in binary systems where material is being transferred from the companion star onto the neutron star. This flow of material is channeled by the magnetic field of the neutron star onto the poles of the star, which creates hot spots on the star's surface. The pulsations are a result of the changing viewing angle of these hot spots as the neutron star rotates. These accreting pulsars are often subdivided into those with a high mass (typically 10–30 solar masses) or low mass (typically less than one solar mass) companion, referred to a HMXB and LMXB, respectively. The anomalous X-ray pulsars are believed to be powered by the decay of their immense magnetic fields (10^{14} – 10^{15} Gauss) (Ref. 18). In addition to pulsars, the X-ray sky contains other highly variable celestial objects that can be used for aspects of spacecraft navigation, including cataclysmic variables (CV) and active galactic nuclei (AGN).

Issues with X-ray Sources. Of the various X-ray sources that exist, X-ray pulsars, including rotation-powered and accretion-powered types, possess the most desirable characteristics for navigation. However, several issues complicate their utilization for navigation solutions. Though nearly all rotation-powered pulsars are constant in intensity, the accreting pulsars and most other X-ray source classes often exhibit highly aperiodic variability in intensity that may compromise their usefulness for precise time and position determination. Some are unsteady, or *transient*, sources with a large range of duty cycles. This phenomenon is due primarily to accretion physics (Ref. 19), and the outburst times of transient sources are often unpredictable. X-ray flares, which are high intensity signals lasting for short periods, are occasionally detected from some sources. Since neutron stars contain a solid crust and a superfluid interior, exchanges of angular momentum between the two materials can cause unpredictable *star-quakes*, or *glitches*, which can significantly alter the spin rates of the stars. A navigation system that utilizes pulsars would have to address

the transient, flaring, and glitching characteristics of these sources. Additionally, as the diffuse X-ray background would be present in all observations, a navigation system that uses pulsed X-ray sources must address the presence of the background noise in its data processing.

While a vast majority of pulsars are detectable at radio wavelengths, only a subset is seen at the optical, X-ray and gamma-ray wavelengths. As X-ray and gamma-rays are difficult to detect on the ground due to their absorption by Earth’s atmosphere, observations in these bands must be made above the atmosphere. In addition, many X-ray sources are faint and require sensitive instruments to be detected. The Crab Pulsar (PSR B0531+21) is the brightest rotation-powered pulsar in the X-ray band, yielding $\sim 2 \times 10^{-9}$ ergs/cm²/s X-ray energy flux in the 2–10 keV band. The next brightest rotation-powered pulsar, PSR B0656+14, is nearly two orders of magnitude fainter than the Crab Pulsar. Pulsars that emit in multiple bands do not necessarily have the same temporal signature in all observable bands. Unlike human-made systems such as GPS, the distances to X-ray sources are not known to an accuracy that would allow absolute range determination between the source and a detector. However, the angular position in the sky can be determined with high precision. Most sources, although located within the Galaxy, are still very far from the solar system. Also, since most sources are clustered along the Milky Way galactic plane, there are a limited number of bright sources that could provide off-axis triangulation for position determination.

Catalogued X-ray Sources. Through a careful literature search, a list of candidate celestial sources can be identified and characterized for potential use in a navigation system, based on criteria such as position knowledge, geometric distribution, brightness, periodic stability, etc. The authors are assembling a catalogue of X-ray sources that will facilitate this assessment. This database currently contains 737 X-ray sources, of which 79 are rotation-powered pulsars. The database includes objects with known accurate angular positions [right ascension (R.A.) and declination (Dec.)], estimated distance, X-ray fluxes and energy ranges, periodicities, and timing stability. Figure 3 plots the X-ray sources from this catalogue using Galactic coordinates. In this figure, the “NS” category includes rotation-powered and anomalous pulsars, and the marker size indicates the relative X-ray intensity of each source.

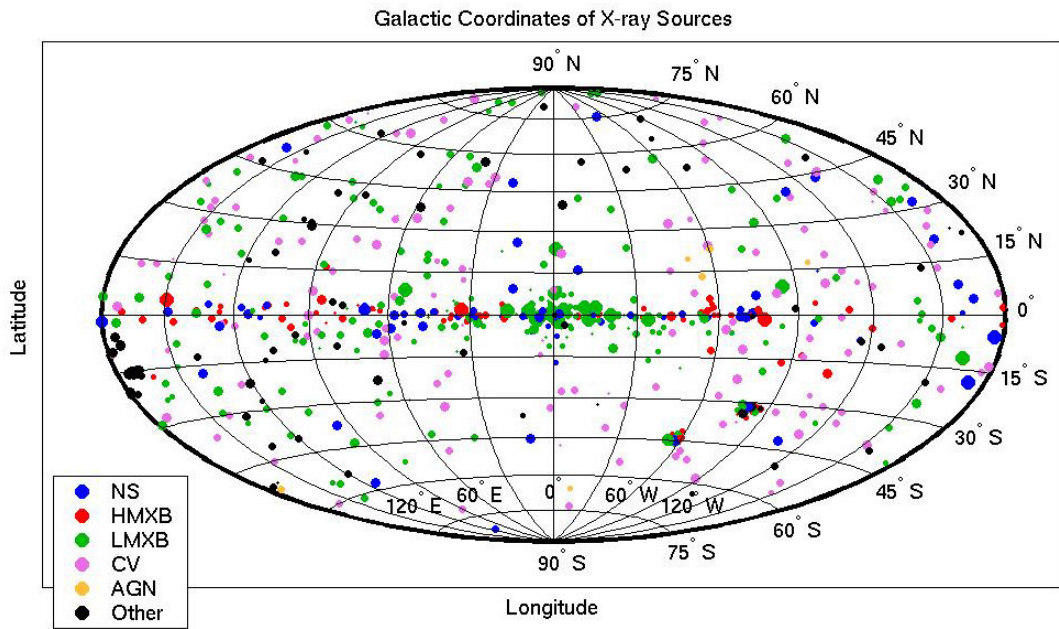


Figure 3. X-ray Sources Plotted in Galactic Coordinates.

X-ray sources exist throughout the X-ray sky, as is evident from Figure 3, although the clustering near the Galactic plane is clear. Distances to X-ray objects range from several to thousands of parsecs. Most rotation-powered pulsars are detected within the Galaxy, however several are located outside the Galaxy in the Magellanic Clouds (two small clusters near Galactic coordinates $120^\circ\text{W}-33^\circ\text{S}$ and $60^\circ\text{W}-45^\circ\text{S}$). Magnetic fields of these objects range from several thousand to 10^{14} Gauss (the Sun's magnetic field is only a few 10s of Gauss). Pulse periods range from 0.0016 to 11.76 seconds for the rotation-powered pulsars, and from 0.034 to 10,000 seconds for accretion-powered pulsars.

As some pulsars have been observed for many years, it has been shown that the stability of their spin rates compares well to the quality of today's atomic clocks. Figures 4 and 5 provide comparison plots of the stability of atomic clocks and several pulsars measured in a third-order Allan Variance. Atomic clocks provide high accuracy references and are typically stable to 1 part in 10^9-10^{15} over a day (Ref. 20). In order to track the motion of radio communication signals from Earth at accuracies of a few tenths of a meter, a spacecraft clock with nanosecond accuracy over several hours is necessary (Ref. 1). This requires the clock to be stable to within one part in 10^{13} . Figure 5 demonstrates that several pulsars compare to typical atomic clock stabilities and meet the requirement for communication signal tracking. The plot in this figure uses data from radio pulsars, however PSR B1937+21 is also detected in X-rays and its X-ray stability is expected to be similar.

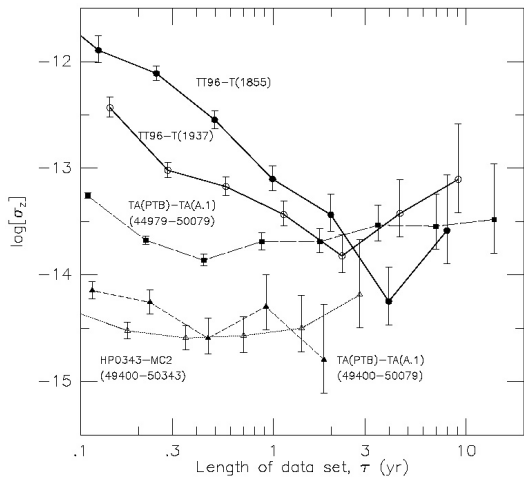


Figure 4. Stability of Atomic Clocks.
(Matsakis, Taylor, and Eubanks, Ref. 20).

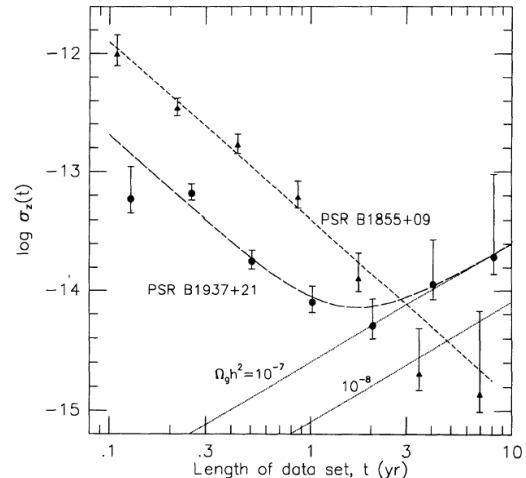


Figure 5. Stability of Pulsars.
(Kaspi, Taylor, and Ryba, Ref. 21).

PULSAR TIMING MODELS

Pulse Profiles

A pulsar pulse profile is a representation of the integrated signal of multiple detected pulses from the pulsar, usually shown as one or two full pulse periods. Pulse profiles vary in amplitude, duration, number of peaks, and stability depending on the nature of the pulsar. This uniqueness aids the identification of an individual source. Typically, standard profile templates are created by observing a specific source over long time spans – many multiples of a pulse period – and *folding*, or averaging synchronously with the pulse period. This folding process produces a pulse profile with a very high signal-to-noise ratio, and characteristics of the pulse can then be determined from this profile, including period length, amplitude, and variability. Figure 6 shows a standard template for the Crab Pulsar (PSR B0531+21) in the X-ray band (2–10 keV). The intensity of the profile is a ratio of count rate relative to average count rate. This image shows two cycles of the pulse, with one main pulse and a secondary pulse at lower amplitude. Figure 7 shows a two-cycle image of the pulse profile of PSR B1509–58.

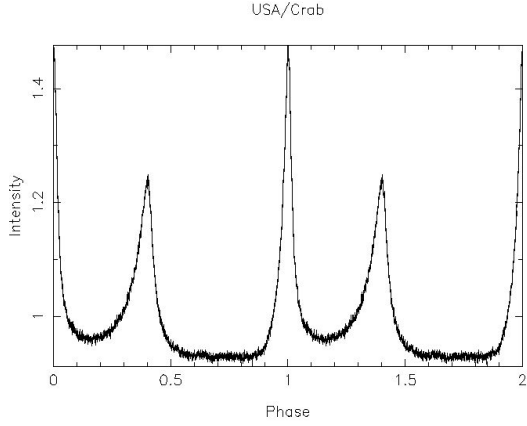


Figure 6. Crab Pulsar Pulse Template.
The period is about 33.4 milliseconds
(epoch 48743.0 MJD) and several period
derivatives have been detected.

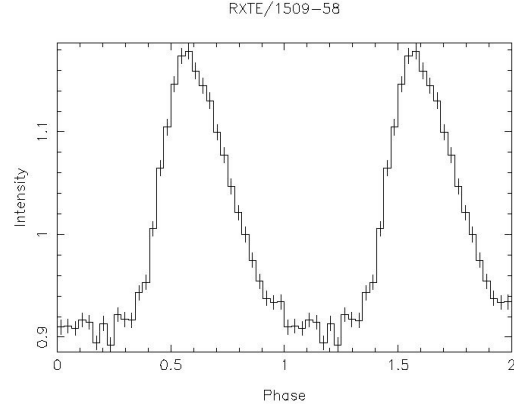


Figure 7. PSR B1509-58 Pulsar Pulse Template.
The period is about 150.23 milliseconds
(epoch 48355.0 MJD).

Pulse Arrival Time Measurement

The fundamental measurable quantity of a pulsar-based navigation system is the arrival time of an observed pulse at the detector. A pulse time of arrival (TOA) measurement is made by observing a pulsar for multiple pulse periods and producing a folded profile. Pulsar signals are timed by comparing measured pulse TOAs with those predicted by a model. The observed profile will differ from the standard profile template, $s(t)$, by several factors, including a bias, b , a scale factor, k , and some random noise $\eta(t)$ (Refs. 19 and 22). For X-ray observations, the random noise is typically dominated by Poisson counting statistics. The relationship between the observed pulse $p(t)$ and the standard template is expressed as,

$$p(t) = b + k \cdot s(t - \tau) + \eta(t) \quad (1)$$

where, τ is the measured time offset between the two profiles.

The observed profile is created via the detection of photons from the pulsar as they arrive at the navigation system's detector. The detector records the time of arrival of each individual X-ray photon with respect to the system clock to high precision (on the order of one microsecond or better). During the total observation time, a large number of photons, N , will have their arrival times recorded. Individual photon arrival times from t_0 to t_N are then converted to their equivalent time in an inertial frame, as described in the sections below. This set of photons is then folded at the predicted pulse period based on the timing model of the pulsar. A binned pulse profile is then constructed by dividing the pulse phase into M equal bins and dropping each of the N photons into the appropriate phase bin.

The TOA is then determined by measuring the phase offset of the observed profile with respect to the high signal-to-noise standard profile template. This is based upon the assumption that, after averaging a sufficiently large number of pulses, a pulse profile recorded in the same energy range is invariant with time. Thus, the phase zero point on the template profile sets the definition of the phase zero for that source. The template can be aligned with an arbitrary point in the profile as phase zero, but two conventions are commonly used. Either the peak of the main pulse can be aligned as the zero phase point, or the profile can be aligned such that the phase of the fundamental component of its Fourier transform is zero. The latter method is preferred (which reduces to the former in the case of a single-symmetric pulse profile) because it is more precise and generally applicable. This latter method also allows for easy construction of standard templates by measuring the phase of the fundamental Fourier component, applying a fractional phase shift to the profile, and then summing many observations to create a high signal-to-noise template profile.

It is important to determine the TOA with an accuracy that is determined by the signal-to-noise ratio of the profile, and not by the choice of the bin size. A standard cross-correlation analysis does not allow this to be easily achieved. However, the method given by Taylor (Ref. 22) is independent of bin size and can be implemented into the navigation system. The technique employs the time shifting property of Fourier transform pairs. The Fourier transform of a function shifted by an amount τ is the Fourier transform of the original function multiplied by a phase factor of $e^{2\pi i f \tau}$, where f is frequency. Since the observed profile differs from the template by a time shift, a scale factor, and random noise, as in Eq. (1), it is straightforward to transform both the profile and the template into the Fourier domain. The parameters in Eq. (1) are then easily determined by a standard least squares fitting method. The final measured TOA of the pulse is then determined by adding the fitted offset τ to the recorded start time of the data set t_0 .

Pulse Phase Timing Models

Due to the periodic nature of the celestial sources, a pulsar phase timing model can be developed, which can be used to predict pulse arrival times. As discussed in Hellings (Ref. 23), Moyer (Refs. 24 and 25), Thomas (Ref. 26), and others (Refs. 27 through 31), in order to compute accurate arrival times of pulses, measurements must be made relative to an inertial frame – a frame unaccelerated with respect to the pulsars. The inertial reference system utilized here has its origin at the solar system barycenter (SSB) and uses the *Temps Dynamique Baricentrique* (TDB), or Barycentric Dynamical Time, as its time coordinate. The position of the SSB is the center of mass of the solar system. Figure 8 shows the relationships of pulses from a pulsar to the SSB inertial frame and to a spacecraft orbiting Earth. The positions of the spacecraft and the center of Earth relative the SSB are shown. Earth-based telescopes or Earth-orbiting spacecraft can reference their observations to specific epochs by initially using terrestrial time standards, such as Coordinated Universal Time (UTC), or *Temps Atomique International* (TAI, International Atomic Time). Standard corrections can then be applied to convert recorded terrestrial time to TDB (Ref. 32).

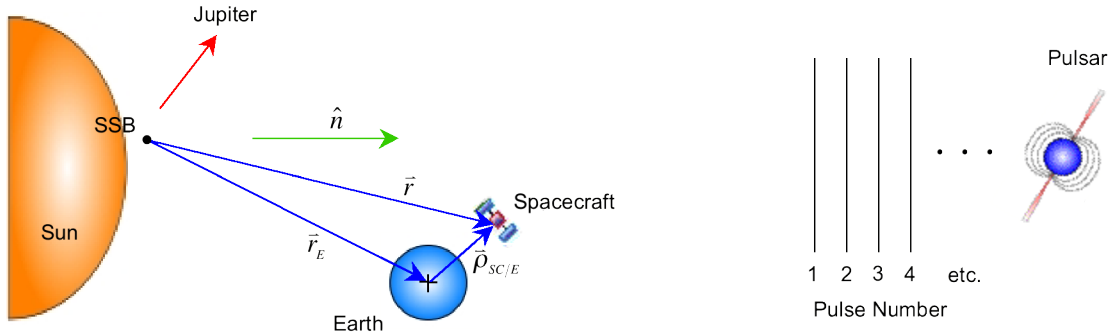


Figure 8. Pulsar Pulse Arrivals Within the Solar System.

The phase, Φ , measured in fractions of the period of arriving pulses, can be specified at the SSB using a pulsar phase model given by

$$\Phi(t) = \Phi(T_0) + f(t - T_0) + \frac{1}{2} \dot{f}(t - T_0)^2 + \frac{1}{6} \ddot{f}(t - T_0)^3 \quad (2)$$

known as the *pulsar spin equation*, where t is the time in TDB, T_0 is the reference epoch, and f, \dot{f}, \ddot{f} are the pulse frequency (usually measured in units of Hz) and its time derivatives. The model parameters for a particular pulsar are generated through repeated observations of the source until a parameter set is created that adequately fits the observed data. The accuracy of the model prediction depends on the quality of the known timing model parameters and on the intrinsic noise of the pulsar rotation. As an example, the Jodrell Bank Observatory performs daily radio observations of the Crab Pulsar, and publishes a monthly ephemeris report (Ref. 33). This published report lists model parameters that describe the pulsar's timing behavior since the beginning of their observations in May 1988.

The pulsar phase model of Eq. (2) allows the determination of the phase of a pulse signal at a future time t , relative to a reference epoch T_0 . The model shown in Eq. (2) utilizes pulse frequency and two derivatives; however, any number of derivatives may be required to accurately model a particular pulsar's timing behavior. Many more parameters may be required for some pulsars, such as those in binary systems but this does not have a negative effect on their ability to be used for navigation.

Time Corrections For Barycenter Offset

The pulsar phase timing model of Eq. (2) provides a method to predict the time of arrival of pulses within the SSB inertial frame. As most observations are typically made on Earth, or on a spacecraft moving about Earth, the data collected while in a moving frame must be transferred to the SSB inertial frame. It is standard to provide model parameters that use the SSB origin as their reference location. In order to compare a measured pulse arrival time at a remote observation station with the predicted time at the SSB origin, the station must project arrival times of photons by its detector onto the SSB origin. This comparison requires time to be transferred from the observation station, or spacecraft, to the SSB, and must at least account for the time delay due to the position offset of the station from the SSB. The General Relativistic theory of gravity provides a method for precisely transferring this time data, and the equations relate the emission time of photons emanating from a source to their arrival time at a station while the photons travel through curved spacetime. The SSB inertial frame was chosen in part due to the simplification of some of the general relativistic equations within this frame. The discussion below describes a method of transferring detected arrival times to the SSB origin.

From Figure 8, it can be seen that from a spacecraft's position \vec{r} relative to the SSB at time t , the offset of time a pulsar signal arrives at a spacecraft compared to its arrival at the SSB to first order is,

$$t_b - t_{obs} = \Delta t = \frac{\hat{n} \cdot \vec{r}}{c} \quad (3)$$

where t_b is the time of pulse arrival at the SSB, t_{obs} is the time of observation at the spacecraft, \hat{n} is the unit direction from the origin to the pulsar, and c is the speed of light. Since many pulsars are so distant from Earth, the unit direction to the pulsars may be considered constant throughout the solar system; however, distant detector positions and any apparent pulsar motion must be included when determining the direction of closer pulsars. Time used in Eq. (3) is referred to as *coordinate time*, or the time measured by a standard clock at rest in the inertial frame. A spacecraft's clock, unless actually at rest (zero-velocity) with respect to the SSB and at the same gravitational potential, does not measure coordinate time. A spacecraft's clock measures *proper time*, or the time a clock measures as it travels along a four-dimensional spacetime path. If a performance goal of such a navigation system is to provide accurate position information on the order of less than 300 meters, then the system must accurately time pulses to better than $1 \mu\text{s}$ ($\approx 300 \text{ m}/c$). To achieve these types of accuracies, general and special relativistic effects on a clock in motion relative to an inertial frame and within a gravitational potential field must be considered. Following the models of Thomas, Moyer, Hellings and others (Refs 23–26, 31, and 34–36), the relationship between differentials of coordinate and proper time for a clock in motion with a maximum error of 10^{-12} s (Ref. 24) is presented as

$$dt = \left[1 + \frac{U}{c^2} + \frac{1}{2} \left(\frac{v}{c} \right)^2 \right] d\tau \quad (4)$$

where τ is the spacecraft clock's proper time, U is the total gravitational potential acting on the spacecraft's clock, and v is the speed of the spacecraft's local frame through the solar system.

By integrating Eq. (4) a solution of the absolute coordinate time relative to the proper time can be determined for a spacecraft clock. Various methods have been employed to solve this integration. Moyer (Refs. 24 and 25) produces a vector-based solution using positions of various planetary bodies and the motion of an atomic clock relative to the SSB. Martin, Torrence, and Misner (Ref. 31) use this solution in a similar derivation. Hellings (Refs. 23 and 27) provides a solution for an Earth-based ground telescope and

its clock used for pulsar timing. A combination of Moyer and Hellings methods is used here to represent a solution for an orbiting spacecraft clock that is used to measure pulsar signal arrival times.

For Earth-orbiting spacecraft, the velocity of the spacecraft's clock, v , with respect to inertial space can be related to Earth coordinate frame using,

$$v^2 = (\bar{v}_E + \dot{\bar{\rho}}_{SC/E}) \cdot (\bar{v}_E + \dot{\bar{\rho}}_{SC/E}) \quad (5)$$

where \bar{v}_E is the velocity of Earth in the SSB frame, and $\dot{\bar{\rho}}_{SC/E}$ is the spacecraft's velocity with respect to Earth. Expanding Eq. (5) and ignoring small terms, Eq. (4) can be rewritten as,

$$(t - t_0) = (\tau - \tau_0) + \int_{\tau_0}^{\tau} \left[\frac{U}{c^2} + \frac{1}{2} \left(\frac{v_E}{c} \right)^2 \right] d\tau + \frac{1}{c^2} (\bar{v}_E \cdot \bar{\rho}_{SC/E}) \quad (6)$$

where $v_E = \|\bar{v}_E\|$. The third term on the right-hand side is often referred to as the *Sagnac effect* (Ref. 35).

Using the following representation of pulsar position, Hellings produces a solution to the second term on the right-hand side of Eq. (6),

$$\bar{D} = \bar{D}_0 + \bar{V}_0(T - T_0) \quad (7)$$

where \bar{D}_0 is assumed to be the position at a fiducial time, T_0 . This model of pulsar motion assumes a constant velocity, \bar{V}_0 , referred to as *proper-motion* of the pulsar, which includes radial and transverse speed terms. Using the additional assumptions that pulsars are very far away from the spacecraft such that $\bar{D}_0 \gg \bar{V}_0(T - T_0)$, the direction to the pulsar is $\hat{n} \approx \bar{D}_0 / \|\bar{D}_0\|$, the values of \bar{V}_0 are small, and that the Sun imposes the primary gravitational field within the solar system, the solution can be reduced to,

$$\Delta t_b = \Delta\tau + \frac{\hat{n} \cdot \bar{r}}{c} - \frac{1}{2c\|\bar{D}_0\|} \left[\|\bar{r}\|^2 - (\hat{n} \cdot \bar{r})^2 \right] + \frac{2\mu_s}{c^3} \left[\ln(\hat{n} \cdot \bar{r}) + \|\bar{r}\| \right] + \frac{1}{c^2} (\bar{v}_E \cdot \bar{\rho}_{SC/E}) \quad (8)$$

where $\mu_s = GM_s$ is the gravitational parameter of the Sun. The second term on the right-hand side of Eq. (8) is the first order *Doppler delay*, and the third term is due to the effects of annual parallax. Together these two terms are referred to as *Roemer delay*. The fourth term is the Sun's *Shapiro delay* (Ref. 37), and the fifth term is the relativistic effects of a portable clock in motion relative to the SSB. With the addition of the fifth term, this equation matches well with those used by Earth-based pulsar timing observations (Refs. 38–42). The interstellar medium dispersion measure term, appearing as a correction for all radio observations, is considered zero in Eq. (8) for high frequency X-ray radiation. Eq. (8) requires accurate ephemeris information to provide the SSB location, the Sun's gravitational parameter, and the velocity of Earth. It is intended for spacecraft in orbit about Earth, and extensions to interplanetary spacecraft can be made through a similar derivation.

Pulse Comparison Summary

The preceding sections provide methods to time observed pulsar pulses and compare to prediction models. This section provides a summary of how to implement this pulse comparison in a manner that would be utilized by a pulsar-based navigation system. A navigation system would be comprised of a sensor that would detect pulsar pulse photons at the spacecraft, a clock onboard the vehicle that would time the photons' arrival, and a database of known timing models for pulsars.

Table 1 provides the steps necessary to complete time transfer of observed pulsar data and comparison to pulsar phase timing models. In order to compute a TOA using Eq. (1) and compare this measured TOA to the predicted TOA of the model in Eq. (2), all time measurements must be converted to the TDB time frame. Also, all pulses must be timed as they would arrive at the SSB origin. Eq. (8) can be used to determine the arrival time at the SSB origin of a pulse detected on the spacecraft. The use of Eq. (8) requires knowledge of spacecraft position and velocity, as well as the gravitational potential acting upon the vehicle.

Table 1
PULSE TIME TRANSFER AND COMPARISON

Process	Steps
Photon Arrival in TDB	<ul style="list-style-type: none"> • Collect and time pulsar X-ray photons at the spacecraft's detector using onboard clock. • Correct spacecraft clock time to terrestrial atomic time standard (i.e. UTC or TAI). • Convert terrestrial atomic time to SSB coordinate system TDB time using standard corrections.
Barycenter Offset Correction	<ul style="list-style-type: none"> • Using spacecraft position and velocity and gravitational potential of solar system, correct measured photon TDB arrival time for offset of vehicle from SSB origin.
TOA Measurement and Offset	<ul style="list-style-type: none"> • Coherently fold photons into an observed pulse profile. • Compare observed pulse profile to standard template profile of pulsar to determine measured TOA of detected pulse in TDB time as it would arrive at SSB origin. • Using pulsar timing model in TDB time, compare predicted TOA of pulse closest to measured TOA to determine difference in pulse arrival time.

PULSAR-BASED NAVIGATION

The preceding section described pulsar timing models and methods to compare the measured pulse TOA to a predicted TOA within an inertial frame. This section provides some additional detail how these comparisons can be used for spacecraft navigation, specifically for determining time and position. Extensions to these concepts can be used to determine vehicle velocity and attitude.

Time

Perhaps the most significant, and the most obvious, benefit of pulsars is to provide accurate atomic clock quality time based solely upon celestial observation. The pulse arrival at the spacecraft provides a periodic signal, which can be used to stabilize an onboard clock. If accurate spacecraft position is known, Eq. (8) can be used to determine the expected arrival of the pulse at the SSB, or conversely Eq. (8) can be used to transform the pulsar arrival model of Eq. (2) to the position of the spacecraft clock. If a spacecraft clock is in error, then the offset of the measured arrival time to the predicted arrival time provides a measure of this clock error.

Assume a spacecraft clock can be represented by the following model,

$$\tau_r = \tau_c + b + k(\tau_c - \tau_0) + \frac{1}{2}j(\tau_c - \tau_0)^2 + \eta(\tau_c) \quad (9)$$

where τ_r is the true time, τ_c is the measured time from the clock, τ_0 is a reference time, b the clock bias, k is the clock rate, j is the clock jitter, and η is the noise within the clock. Given estimates of b , k , and j , a Kalman filter can be created using this clock model. Hanson (Ref. 14) provides a method of correcting clock time using a phase-locked loop. In this feedback loop, the phase difference between the local clock's oscillator and the reference signal from the pulsar is driven towards zero. Using repeated pulsar observations, the phase differences are continuously computed and any local clock errors are removed.

Position

Because of the unique signatures of pulsars, it is possible to determine position of a spacecraft. Position is determined relative to a desired inertial frame. Although the SSB provides one such frame and reference origin, it is often more useful for mission operations to also relate vehicle position to Earth's position. Two methods of position determination relative to Earth are provided below. Methods for determining position of spacecraft on interplanetary missions can be extended from the examples below.

$$\begin{bmatrix} (\delta t_b - \delta \tau)_1 \\ (\delta t_b - \delta \tau)_2 \\ \cdot \\ \cdot \\ (\delta t_b - \delta \tau)_k \end{bmatrix} = \begin{bmatrix} \bar{N}_1 \\ \bar{N}_2 \\ \cdot \\ \cdot \\ \bar{N}_k \end{bmatrix} \delta \bar{r} \quad (14)$$

If no errors in modeling or measurement are present, then Eq. (14) solves directly for accurate position offsets. However, errors do remain which limit the performance of this system; δt contains errors in pulsar timing models, $\delta \tau$ contains system level timing errors and pulse signal timing errors, and these errors along with any errors in parameters of \bar{N} , including pulsar position uncertainty and Earth ephemeris accuracy, contribute to the errors in $\delta \bar{r}$. A phase cycle ambiguity is still present, as these equations only can relate to a fraction of a cycle and not which *specific* cycle is being detected. Additionally, vehicle motion that is significant during the time span between current time and pulse arrival time must be addressed in an implementation of this delta position estimate system. A Kalman filter incorporating vehicle dynamics and a measurement model from Eq. (14) can be used to successfully update vehicle position estimates. Additional complexity is added if one chooses to incorporate binary pulsar observations, and these extra terms must be added to Eq. (14) (Refs. 43, 44, and 45).

Absolute Position Determination. Although determining an offset to an estimated position is useful for some systems, navigation systems that can determine absolute position using no prior knowledge are often very desirable. A navigation system that can operate in this absolute, or *cold-start*, mode does not require any assistance from outside sources, such as ground-based radar, and are very advantageous after abnormal circumstances, such as a computer reset after a vehicle power failure.

To determine absolute position from signals of a pulsar it is necessary to track the entire phase of the signals, not simply the peak amplitudes. By tracking the phase of several pulsars and including the pulsar line-of-sight directions, it is possible to determine the unique set of cycles that satisfies the combined information. This unique set of cycles is then used to determine position relative to the SSB. Multiple simultaneous pulsar observations may be required for this method. This identification process is very similar to the GPS integer cycle *ambiguity-resolution* method. Offering an advantage over GPS, pulsars can provide many different cycle lengths, some very small (few milliseconds) to very large (many thousand of seconds), which assists the pulse cycle resolution method.

Numerical Study

Using data recorded by the NRL USA experiment, a pulsar-based navigation system's performance can begin to be assessed. On December 24, 1999 starting at 9:06:12.9 (UTC), the USA detector was pointed to observe the Crab pulsar, located at $05^{\text{h}}34^{\text{m}}31.972^{\text{s}}$ R.A. (J2000) and $22^{\circ}00'52.069''$ Dec. (J2000). An observation of 695.89 seconds was recorded, including time-tagged X-ray photon counts and *ARGOS* satellite one-second position values. Using the Crab pulsar pulse period, these recorded data were then folded to produce an observed profile. Prior to this specific observation, several separate observations were folded to produce a standard template profile with a high signal-to-noise ratio for the Crab pulsar. Using both the observed profile and the template profile in the method described in the Pulse Arrival Time Measurement section above, an observation pulse TOA = $51536.385663752852 \pm 6.0185 \times 10^{-11}$, in Modified Julian Date (MJD), was generated. This pulse TOA represents the arrival time of the peak of the first pulse within the observation window, which for this observation contained approximately 20770 pulse cycles. The error in the TOA ($\pm 6.0185 \times 10^{-11}$ days) represents the uncertainty in aligning the observed and template profiles and is related to the signal-to-noise ratio of the observed profile.

In the process of computing the pulse TOA, the analysis tool corrects the spacecraft recorded photon arrival time to their arrival time at the SSB. This process uses an expression similar to Eq. (8) along with

the recorded spacecraft position and velocity from *ARGOS* navigation data. Thus, the TOA is the arrival time at the SSB origin of the measured pulse detected at the USA detector. The Crab pulsar's timing model has been determined by the Jodrell Bank Observatory (Ref. 20) as frequency = 29.8467040932 Hz (or period = 0.0335045369458 seconds) and frequency first-derivative = $-3.7461268 \times 10^{-10}$ Hz/s at epoch $T_0 = 51527.0000001373958$ (MJD). With this predetermined Crab pulsar timing model, the predicted arrival time of the same pulse using the model of Eq. (2) is pulse number 24203206 at TOA = 51536.385663753211 (MJD). The difference between the measured and the predicted TOA is calculated to be -31.018 ± 5.2 microseconds.

Position information can now be derived from this measured arrival time difference. If the assumption is made that this difference is based solely upon vehicle position offset, the error in spacecraft position can be deduced from the pulsar pulse observation. From Eq. (12) and the estimated distance to the Crab pulsar of 2 kiloparsecs, a position offset of -9299.1 ± 1559 m along the direction of the Crab pulsar is determined.

The delta position of 9.3 km represents the estimate offset a pulsar-based navigation system would produce based upon this single TOA measurement. During the course of the USA experiment mission, NRL conducted a parallel study of a ground-based navigation system. This study has reported that the recorded *ARGOS* satellite navigation system position was in error as much as 15 km during several USA observations in January 2000. With these magnitudes of position error discovered for January 2000, it is likely that they existed for the observations completed during December 1999, which would account for much of the position offset determined from the measured TOA above.

The estimated position offset error of 1.6 km (from 5.2 microseconds) represents the accuracy of the TOA calculation. In determining this position offset, it was assumed that there was no known timing error present in the USA experiment data collection, that the pulsar timing model is accurate, and that the pulsar position is known accurately. Any errors in these components would affect the accuracy of this computed position offset. However, the reported accuracy of the timing model parameters provided by the Jodrell Bank Observatory is 60 microseconds for the month of December 1999. Also the USA experiment was designed to maintain a 32-microsecond photon bin timing accuracy, and fractions of the bin size were used for increased time resolution. Some of this pulsar model and photon timing error may be present in these calculations, which affects the accuracy of the TOA measurement and consequently the position accuracy.

CONCLUSION

Rotation-powered and accretion-powered pulsars represent a small, but important, subset of all possible X-ray sources. These unique celestial sources provide pulsed radiation that can be utilized in a navigation system for spacecraft. Given their large distances from Earth, pulsars provide good signal coverage for operations within the solar system, and conceivably, the Galaxy. Issues with these sources exist that make their use complicated. However, further algorithmic and experimental study may address these complications. With the potential ability to generate a *complete* navigation solution, including time, position, and attitude over large distances from Earth, X-ray pulsars remain attractive for creating a new celestial-based spacecraft navigation system.

ACKNOWLEDGEMENTS

The authors would like to thank those at the Naval Research Laboratory for their assistance with this project, including Zachary Fewtrell, Jon Determan, Lev Titarchuk, and Daryl Yentis. They also thank Yong H. Kim of Saddleback College, Larry Vallot of the Honeywell Technology Labs, Stuart Bale of University of California, Berkeley, and David Nice of Princeton University for their many helpful discussions and insights. Sheikh and Pines express their gratitude to the Metropolitan Washington, DC Chapter of the ARCS Foundation for providing a majority of the support for this research through their fellowship program. They also express appreciation to the Aerospace Engineering Department's Gustave J. Hokenson Fellowship for its support. This work was supported in part by the Office of Naval Research.

REFERENCES

1. Melbourne, W. G., "Navigation Between the Planets", *Scientific American*, Vol. 234, No. 6, June 1976, pp. 58–74.
2. Jordan, J. F., "Navigation of Spacecraft on Deep Space Missions", *Journal of Navigation*, Vol. 40, January 1987, pp. 19–29.
3. Weeks, C. J., and Bowers, M. J., "Analytical Models of Doppler Data Signatures", AAS Paper 94–178, *Advances in Astronautical Sciences*, Vol. 87, No. 2, 1994, pp. 1187–1198.
4. Gounley, R., White, R., and Gai, E., "Autonomous Satellite Navigation by Stellar Refraction", *Journal of Guidance and Control*, Vol. 7, No. 2, March–April 1984, pp. 129–134.
5. Folta, D. C., et al., "Autonomous Navigation Using Celestial Objects", AAS Paper 99-439, American Astronautical Society Astrodynamics Specialist Conference, August 1999, pp. 2161–2177.
6. Hewish, A., et al., "Observation of a Rapidly Pulsating Radio Source", *Nature*, Vol. 217, February 1968, pp. 709–713.
7. Manchester, R. N., et al., "The Parkes Multi-beam Pulsar Survey", *Monthly Notices of the Royal Astronomical Society*, Vol. 328, 2001, pp. 17–35.
8. Chandra X-ray Observatory, "Time Lapse Movies of Crab Nebula", NASA/CXC/ASU/J.Hester et al., Online: Available at <http://chandra.harvard.edu/photo/2002/0052/movies.html>, [cited June 2003].
9. Downs, G. S., "Interplanetary Navigation Using Pulsating Radio Sources", *NASA Technical Reports N74-34150*, October 1, 1974, pp. 1–12.
10. Wallace, K., "Radio Stars, What They are and The Prospects for their Use in Navigational Systems", *Journal of Navigation*, Vol. 41, No. 3, September 1988, pp. 358–374.
11. Shearer, A., Golden, A., and Beskin, G., "Implications of the Optical Observations of Isolated Neutron Stars", *Pulsar Astronomy – 2000 and Beyond*, Eds. M. Kramer, N. Wex, and R. Wielebinski, Astronomical Society of Pacific Conference Series, Vol. 202, 1999, pp. 307–310.
12. Chester, T. J., and Butman, S. A., "Navigation Using X-Ray Pulsars", *NASA Technical Reports N81-27129*, June 15, 1981, pp. 22–25.
13. Wood, K. S., "Navigation Studies Utilizing the NRL-801 Experiment and the ARGOS Satellite", *Small Satellite Technology and Applications III*, Ed. B. J. Horais, SPIE Proceedings, Vol. 1940, 1993, pp. 105–116.
14. Hanson, J.E., "Principles of X-ray Navigation", Doctoral Dissertation, Stanford University, March 1996.
15. Wood, K. S., et al., "The USA Experiment on the ARGOS Satellite: A Low Cost Instrument for Timing X-ray Binaries", *EUV, X-Ray, and Gamma-Ray Instrumentation for Astronomy V*, Eds. O. H. Siegmund & J. V. Vallerga, SPIE Proceedings, Vol. 2280, 1994, p. 19.
16. Wood, K. S., et al., "The USA Experiment on the ARGOS Satellite: A Low Cost Instrument for Timing X-ray Binaries", *The Evolution of X-ray Binaries*, Eds. S. S. Holt and C. S. Day, American Institute of Physics Proceedings, No. 308, 1994, p. 561–564.
17. Ray, P. S., et al., "The USA X-ray Timing Experiment", *American Institute of Physics Conference Proceedings*, Vol. 599, 2001, p. 336.
18. Thompson, C., and Duncan, R. C., "The Soft Gamma Repeaters As Very Strongly Magnetized Neutron Stars. Part II. Quiescent Neutrino, X-ray, and Alfvén Wave Emission", *Astrophysical Journal*, Vol. 473, 10 December 1996, pp. 322–342.
19. Taylor, J. H., and Stinebring, D. R., "Recent Progress in the Understanding of Pulsars", *Annual Review of Astronomy and Astrophysics*, Vol. 24, 1986, pp. 285–327.
20. Matsakis, D. N., Taylor, J. H., and Eubanks, T. M., "A Statistic for Describing Pulsar and Clock Stabilities", *Astronomy and Astrophysics*, Vol. 326, 1997, pp. 924–928.
21. Kaspi, V. M., Taylor, J. H., and Ryba, M. F., "High-Precision Timing of Millisecond Pulsars. III. Long-Term Monitoring of PSRs B1855+09 and B1937+21", *Astrophysical Journal*, Vol. 428, June 1994, pp. 713–728.
22. Taylor, J. H., "Pulsar Timing and Relativistic Gravity", *Philosophical Transactions Royal Society of London*, Vol. 341, 1992, pp. 117–134.

23. Hellings, R. W., “Relativistic Effects in Astronomical Timing Measurements”, *Astronomical Journal*, Vol. 91, No. 3, March 1986, pp. 650–659.
24. Moyer, T. D., “Transformation From Proper Time on Earth to Coordinate Time in Solar System Barycentric Space-Time Frame of Reference, Part 1”, *Celestial Mechanics*, Vol. 23, 1981, pp. 33–56.
25. Moyer, T. D., “Transformation From Proper Time on Earth to Coordinate Time in Solar System Barycentric Space-Time Frame of Reference, Part 2”, *Celestial Mechanics*, Vol. 23, 1981, pp. 57–68.
26. Thomas, J. B., “Reformulation of the Relativistic Conversion Between Coordinate Time and Atomic Time”, *Astronomical Journal*, Vol. 80, No. 5, May 1975, pp. 405–411.
27. Backer, D. C., and Hellings, R. W., “Pulsar Timing and General Relativity”, *Annual Review of Astronomy and Astrophysics*, Vol. 24, 1986, pp. 537–575.
28. Stumpff, P., “On the Computation of Barycentric Radial Velocities with Classical Perturbation Theories”, *Astronomy and Astrophysics*, Vol. 56, 1977, pp. 13–23.
29. Stumpff, P., “The Rigorous Treatment of Stellar Aberration and Doppler Shift, and the Barycentric Motion of the Earth”, *Astronomy and Astrophysics*, Vol. 78, 1979, pp. 229–238.
30. Lorimer, D. R., “Binary and Millisecond Pulsars at the New Millennium”, *Living Review in Relativity*, Max Planck Institute for Gravitational Physics, Albert Einstein Institute, Germany, June 2001.
31. Martin, C. F., Torrence, M. H., and Misner, C. W., “Relativistic Effects on an Earth-Orbiting Satellite in the Barycenter Coordinate System”, *Journal of Geophysical Research*, Vol. 90, No. B11, September 1985, pp. 9403–9410.
32. Seidelmann, P. K., Ed., *Explanatory Supplement to the Astronomical Almanac*, University Science Books, 1992.
33. Lyne, A. G., Jordan, C. A., and Roberts, M. E., “Jodrell Bank Crab Pulsar Timing Results, Monthly Ephemeris”, [online], URL: <http://www.jb.man.ac.uk/~pulsar/crab.html>, University of Manchester, [cited 13 August 2002].
34. Ashby, N., and Allan, D. W., “Coordinate Time On and Near the Earth”, *Physical Review Letters*, Vol. 53, No. 19, November 1984, p. 1858.
35. Parkinson, B. W. and Spilker, J. J. Jr., Eds., *Global Positioning System: Theory and Applications, Volume I*, AIAA, 370 L’Enfant Promenade, SW, Washington, DC, 1996.
36. Parkinson, B. W. and Spilker, J. J. Jr., Eds., *Global Positioning System: Theory and Applications, Volume II*, AIAA, 370 L’Enfant Promenade, SW, Washington, DC, 1996.
37. Shapiro, I. I., “Fourth Test of General Relativity”, *Physical Review Letters*, Vol. 13, No. 26, December 1964, pp. 789–791.
38. Rawley, L. A., Taylor, J. H., and Davis, M. M., “Fundamental Astrometry and Millisecond Pulsars”, *Astrophysical Journal*, Vol. 326, March 1988, pp. 947–953.
39. Kaspi, V. M., “High-Precision Timing of Millisecond Pulsars and Precision Astrometry”, proceedings of 166th Symposium of the International Astronomical Union, Eds. E. Hog and P. Kenneth Seidelmann, August 1994, pp 163–174.
40. Bell, J. F., “Radio Pulsar Timing”, *Advances in Space Research*, Vol. 21, No. 1/2, 1998, pp. 137–147.
41. Manchester, R. N., and Taylor, J. H., *Pulsars*, W. H. Freeman and Company, 1997.
42. Lyne, A. G., and Graham-Smith, F., *Pulsar Astronomy*, Cambridge University Press, 2nd Edition, 1998.
43. Taylor, J. H., and Weisberg, J. M., “Further Experimental Tests of Relativistic Gravity Using the Binary Pulsar PSR 1913+16”, *Astrophysical Journal*, Vol. 345, October 1989, pp. 434–450.
44. Blandford, R. and Teukolsky, S. A., “Arrival-Time Analysis for a Pulsar in a Binary System”, *Astrophysical Journal*, Vol. 205, April 1976, pp. 580–591.
45. Kopeikin, S. M., “Millisecond and Binary Pulsars as Nature's Frequency Standards - II. The Effects of Low-Frequency Timing Noise on Residuals and Measured Parameters”, *Monthly Notices of the Royal Astronomical Society*, Vol. 305, 1999, pp. 563–590.